Supplementary Information

Electrically controlled valley states in bilayer graphene

Afsal Kareekunnan,[1] Manoharan Muruganathan,[1,*] and Hiroshi Mizuta[1,2]

[1] *School of Materials Science, Japan Advanced Institute of Science and Technology, 1-1 Asahidai, Nomi, 923-1292, Japan*
[2] *Hitachi Cambridge Laboratory, Hitachi Europe Ltd., Cavendish Laboratory, JJ Thomson Avenue, Cambridge CB3 0HE, UK*

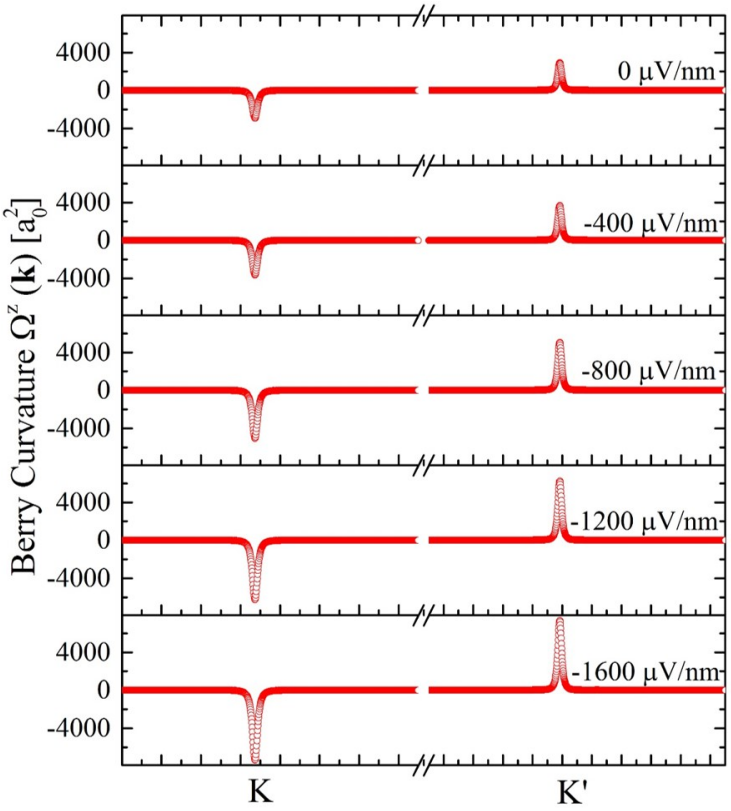

Supplementary Fig. 1 – **a-e** Berry curvature plot for bilayer graphene at different negative electric fields. The Berry curvature at both K and K′ high symmetry points does not show any sign change with the increase in the electric field. The increase in the magnitude of the Berry curvature is the result of growing asymmetry in the system with the increase in electric field strength.

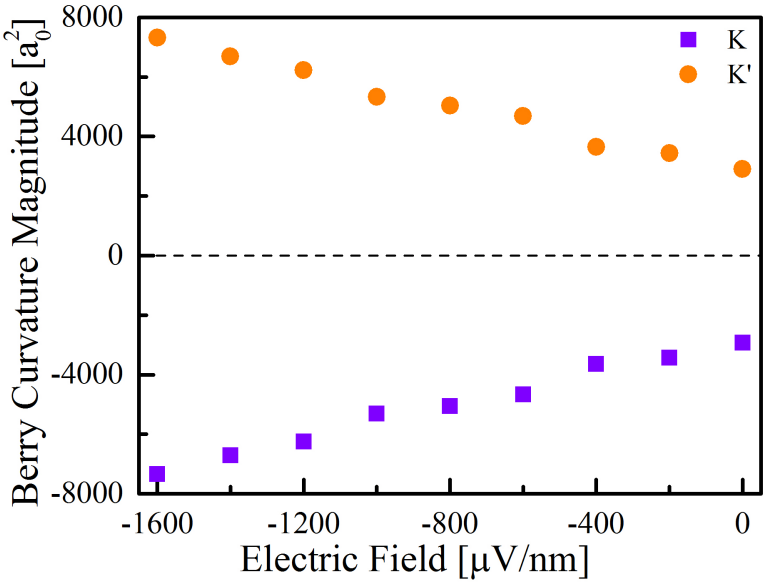

Supplementary Fig. 2 – The magnitude of the Berry curvature at both K and K′ valleys for different negative out-of-plane electric fields.

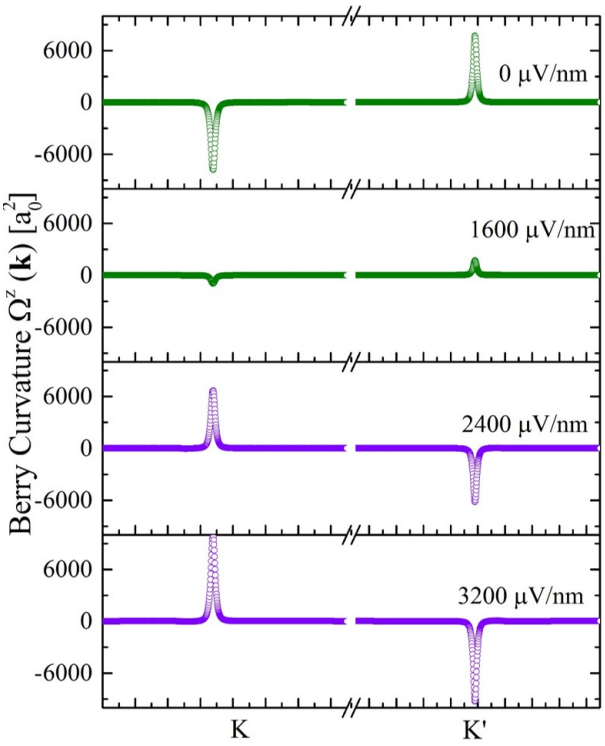

Supplementary Fig. 3 – Berry curvature calculated at different positive electric fields using QUANTUM ESPRESSO (see Methods, Supplementary Information). **a** As observed in the calculations performed using SIESTA (Fig. 2a, main text), a non-zero Berry curvature with opposite values at K and K′ valleys is observed, validating the argumentation of inbuilt inter-layer charge asymmetry persistent in neutral bilayer graphene as a result of charge transfer. **b** The increase in the electric field reduces the magnitude of the Berry curvature and hence the charge asymmetry. **c** Further increase in the magnitude of the electric field reverses the polarity of the Berry curvature at both K and K′ valleys. This implies that the charge asymmetry shifts to the opposite layer beyond a threshold electric field. **d** Increasing the electric field strength beyond the threshold electric field increases the magnitude of the Berry curvature as a consequence of the increase in charge asymmetry.

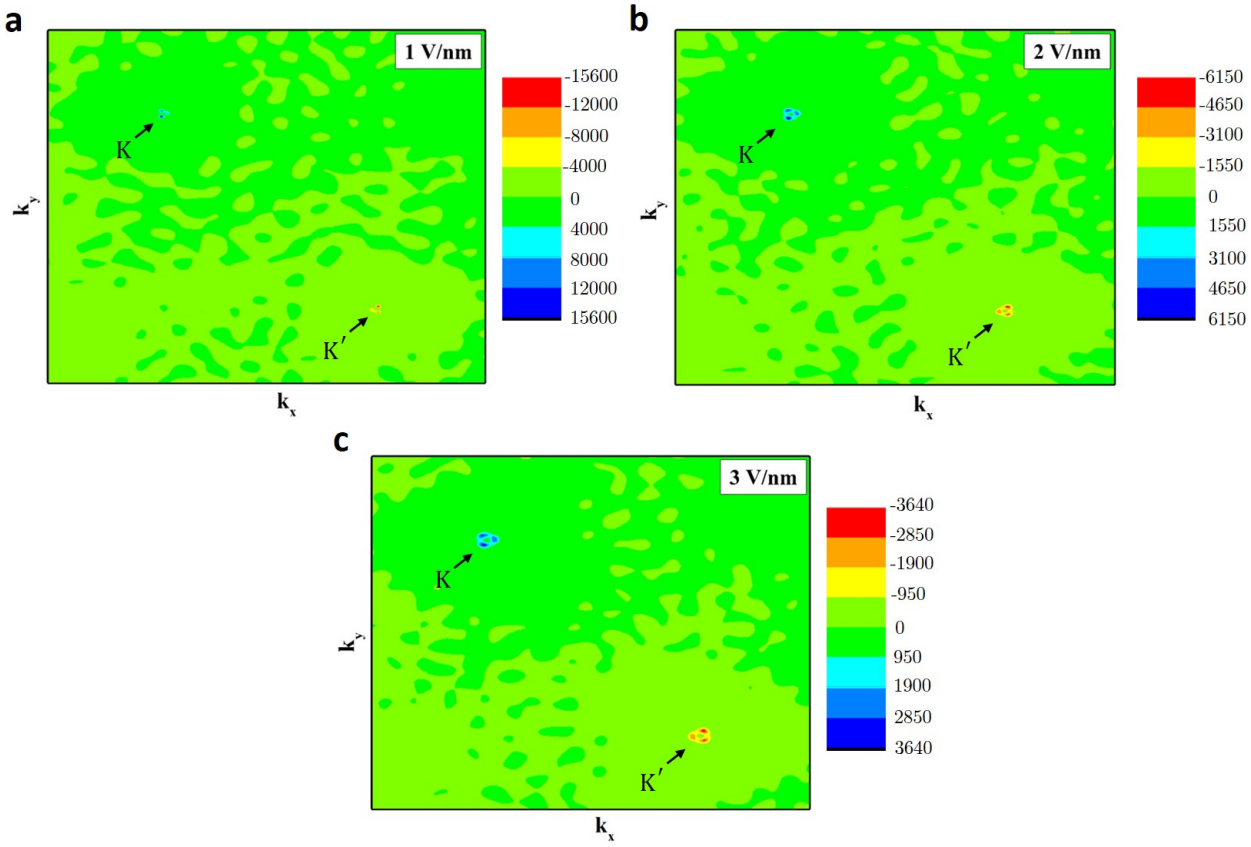

Supplementary Fig. 4 – Berry curvature plotted in the 2D k-space **a** for 1 V/nm, **b** for 2 V/nm, and **c** for 3 V/nm. At higher electric fields, the Berry curvature delocalizes and spreads across the 2D k-space with the increase in the strength of the applied out-of-plane electric field.

Supplementary Note 1

Berry curvature for the nth band is defined as

$$\mathbf{\Omega}_n(\mathbf{k}) = i\frac{\hbar^2}{m^2}\sum_{n\neq n'}\frac{\langle u_{n,\boldsymbol{k}}|\,\hat{\mathbf{p}}\,|u_{n',\boldsymbol{k}}\rangle \times \langle u_{n',\boldsymbol{k}}|\,\hat{\mathbf{p}}\,|\,\rangle\, u_{n,\boldsymbol{k}}}{[\varepsilon_n - \varepsilon_{n'}]^2} \tag{1}$$

where, $\hat{\mathbf{p}}$ is the momentum operator, $|u_{n,\boldsymbol{k}}\rangle$ is the periodic part of the Bloch function and ε_n is the energy of the n^{th} Bloch band. The summation runs over all the bands including the un-occupied bands. The total Berry curvature is the sum over all the occupied bands, i.e.,

$$\mathbf{\Omega}(\mathbf{k}) = \sum_n f_n \mathbf{\Omega}_n(\mathbf{k}) \tag{2}$$

where f_n is the Fermi-Dirac distribution.

But taking the derivative of the periodic part of the Bloch function (Eq. (1)) makes the calculation cumbersome. Thus we rely on the more accurate Wannier interpolation scheme, where the Berry curvature, calculated in terms of the Wannier functions [1] using finite differences is defined as,

$$\mathbf{\Omega}(\mathbf{k}) = \sum_n f_n \overline{\mathbf{\Omega}}^H_{nn} + \sum_{n,m}(f_m - f_n)\mathbf{D}^H_{nm} \times \overline{\mathbf{A}}^H_{nm} + \mathbf{\Omega}^{DD} \tag{3}$$

where $\overline{O}^H = U^\dagger O^W U$ represent the components which transform covariently from Wannier gauge (W) to Hamiltonian gauge (H) under unitary transformation U ; and $\boldsymbol{D}^H_{nm} = \frac{(U^\dagger \nabla H^W U)_{nm}}{\varepsilon_m - \varepsilon_n}(1-\delta_{nm})$. The last term is defined as

$$\mathbf{\Omega}^{DD} = \frac{i}{2}\sum_{n,m}(f_n - f_m)\frac{(U^\dagger \nabla H^W U)_{nm} \times (U^\dagger \nabla H^W U)_{nm}}{(\varepsilon_m - \varepsilon_n)^2} \tag{4}$$

Here, H^W is the Hamiltonian in Wannier representation and ε_n is the energy of the n^{th} band.

The summation runs over all the Wannier states, which is, all the occupied and two un-occupied states in our case. The term $(f_n - f_m)$ in Eq. (4) tells that a pair of occupied states or un-occupied states have negligible contribution to the total Berry curvature. Thus, a pair of bands, one of them occupied and another one un-occupied contribute extensively to the total Berry curvature. In that case, ε_m and ε_n are the energies of these occupied and un-occupied valleys respectively. Hence increasing the band gap results in the decrease in total Berry curvature because Berry curvature is inversely proportional to the square of the energy difference between conduction band minimum and valence band maximum.

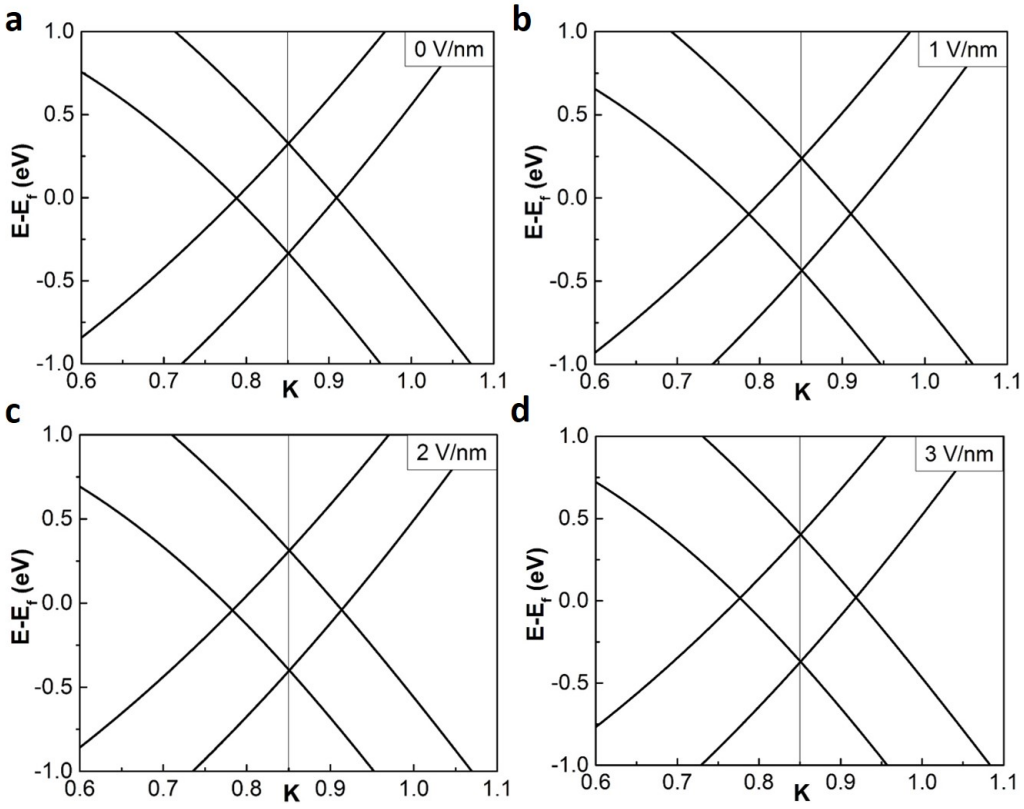

Supplementary Fig. 5 – Band structure calculations for AA-stacked bilayer graphene near the Fermi level around the K valley **a** for 0 V/nm **b** for 1 V/nm **c** for 2 V/nm **d** for 3 V/nm. No band gap opening was observed in spite of the application of an out-of-plane electric field which induces a potential difference between the layers. This signifies that the layer symmetry in AA-stacked bilayer graphene remains unaltered regardless of the application of an out-of-plane electric field.

Methods

Ab initio calculations are performed using QUANTUM ESPRESSO [2] which uses plane-wave basis. PBE exchange-correlation functional [3] which employs Generalized Gradient Approximation (GGA) is used all the calculations. A norm-conserving pseudo-potential with kinetic energy cutoff for wave functions of 80 Ry is used (320 Ry for charge density cutoff). In order to procure optimum interlayer distance between the two graphene layers, semi-empirical Grimme's DFT-D2 [4] van der Waals correction is employed. The Berry curvature calculations are performed using the WANNIER90 package which follows the Wannierization procedure [5]. A total of 10 Wannier functions are constructed on a fine Monkhorst-Pack grid of dimension 72 x 72 x 1. In the disentanglement procedure, the Wannier spread is converged down to 10^{-10} Å^2 in less than 600 iterations.

* E-mail: mano@jaist.ac.jp

[1] Xinjie Wang, Jonathan R. Yates, Ivo Souza and David Vanderbilt, *Ab initio* calculation of the anomalous Hall conductivity by Wannier interpolation. Phys. Rev. B **74**, 195118 (2006).

[2] Paolo Giannozzi, Stefano Baroni, Nicola Bonini, Matteo Calandra, Roberto Car, Carlo Cavazzoni, Davide Ceresoli, Guido L Chiarotti, Matteo Cococcioni, Ismaila Dabo, Andrea Dal Corso, Stefano de Gironcoli, Stefano Fabris, Guido Fratesi, Ralph Gebauer, Uwe Gerstmann, Christos Gougoussis, Anton Kokalj, Michele Lazzeri, Layla Martin-Samos, Nicola Marzari, Francesco Mauri, Riccardo Mazzarello, Stefano Paolini, Alfredo Pasquarello, Lorenzo Paulatto, Carlo Sbraccia, Sandro Scandolo, Gabriele Sclauzero, Ari P Seitsonen, Alexander Smogunov, Paolo Umari and Renata M Wentzcovitch, QUANTUM ESPRESSO: a modular and open-source software project for quantum simulations of materials. J. Phys.: Condens. Matter **21**, 395502 (2009).

[3] John P. Perdew, Kieron Burke and Matthias Ernzerhof, Generalized Gradient Approximation Made Simple. Phys. Rev. Lett. **77**, 3865 (1996).

[4] Stefan Grimme, Semiempirical GGAtype density functional constructed with a longrange dispersion correction. J. Comp. Chem. **27**, 1787 (2006).

[5] Ivo Souza, Nicola Marzari and David Vanderbilt, Maximally localized Wannier functions for entangled energy bands. Phys. Rev. B **65**, 035109 (2001).